Optics Letters

One-dimensional photonic crystal slot waveguide for silicon-organic hybrid electro-optic modulators

Hai Yan,[1,†] Xiaochuan Xu,[2,†] Chi-Jui Chung,[1,†] Harish Subbaraman,[2,3] Zeyu Pan,[1] Swapnajit Chakravarty,[2] and Ray T. Chen[1,2,*]

[1]Department of Electrical and Computer Engineering, The University of Texas at Austin, Austin, Texas 78758, USA
[2]Omega Optics Inc., 8500 Shoal Creek Blvd., Austin, Texas 78759, USA
[3]Department of Electrical and Computer Engineering, Boise State University, Boise, Idaho 83725, USA
*Corresponding author: raychen@uts.cc.utexas.edu

Received 26 September 2016; revised 28 October 2016; accepted 30 October 2016; posted 1 November 2016 (Doc. ID 276393); published 21 November 2016

In an on-chip silicon-organic hybrid electro-optic (EO) modulator, the mode overlap with EO materials, in-device effective r_{33}, and propagation loss are among the most critical factors that determine the performance of the modulator. Various waveguide structures have been proposed to optimize these factors, yet there is a lack of comprehensive consideration on all of them. In this Letter, a one-dimensional (1D) photonic crystal (PC) slot waveguide structure is proposed that takes all these factors into consideration. The proposed structure takes advantage of the strong mode confinement within a low-index region in a conventional slot waveguide and the slow-light enhancement from the 1D PC structure. Its simple geometry makes it robust to resist fabrication imperfections and helps reduce the propagation loss. Using it as a phase shifter in a Mach–Zehnder interferometer structure, an integrated silicon-organic hybrid EO modulator was experimentally demonstrated. The observed effective EO coefficient is as high as 490 pm/V. The measured half-wave voltage and length product is less than 1 V · cm and can be further improved. A potential bandwidth of 61 GHz can be achieved and further improved by tailoring the doping profile. The proposed structure offers a competitive novel phase-shifter design, which is simple, highly efficient, and with low optical loss, for on-chip silicon-organic hybrid EO modulators. © 2016 Optical Society of America

OCIS codes: (250.2080) Polymer active devices; (130.4110) Modulators; (130.5296) Photonic crystal waveguides.

https://doi.org/10.1364/OL.41.005466

The high speed, high efficiency integrated electro-optic (EO) modulator built on silicon substrate is an important building block for short-reach optical interconnect [1]. Since the second-order nonlinearity ($\chi^{(2)}$) of silicon is negligible, most silicon-integrated EO modulators rely on the plasma dispersion effect, in which the change of free carrier concentration induces the change of refractive index in silicon waveguides [2,3]. The bandwidths and modulation efficiencies of these modulators are therefore limited by the free carrier dynamics. On the other hand, polymer EO materials possess intriguing second-order nonlinear optical properties, such as high nonlinear coefficient and ultrafast response time, and can be applied easily through spin-casting [4–6]. The silicon-organic hybrid platform combines advantages of both silicon photonic and polymer materials, enabling large modulation bandwidth and small voltage-length product simultaneously in EO modulation applications [7–9].

Silicon-organic hybrid EO modulators based on various phase-shifter designs have been reported in recent years. These structures include slot waveguides [10–13], two-dimensional (2D) slot photonic crystal (PC) waveguides [14–16], and one-dimensional (1D) PC waveguides [17]. High modulation efficiency has been achieved in slot waveguides because of the strong confinement of the optical mode in low-index slot regions infiltrated with EO materials, which leads to large mode volume overlap with an EO polymer. Slow-light waveguides, like 2D slot PC waveguides, have also been proposed, which utilize the slow-light effect and greatly enhance effective r_{33} [14–16]. In 2D slot PC waveguides, however, the optical loss in a slow-light region and its robustness against fabrication variations is a concern, especially in a dispersion-engineered PC slot waveguide, considering its complicated structure and delicate arrangement of the PC holes [15]. Reports have shown that the propagation loss in a 2D PC slot is very sensitive to slot width variations [18]. In Ref. [17], a novel 1D PC structure is introduced. With proper use of the air band in the PC, the structure achieves high mode overlap ($\sigma = 0.67$) and slow-light enhancement simultaneously, although the poling efficiency of the EO polymer between the pillars is relatively low, because voltage drop in this area is reduced by the silicon pillars. In reality, the mode overlap with EO material, effective r_{33} (proportional to slow-light enhancement), and propagation loss are among the most important factors for a silicon-organic hybrid EO modulator, yet there is a lack of comprehensive consideration of all these factors.

In this Letter, we propose a new slow-light slot waveguide with 1D PC structure that takes all these factors into consideration. We further define a comprehensive figure-of-merit to compare it with previous reported modulator phase-shifter designs. The proposed 1D PC structure takes advantage of the strong mode confinement in the low-index region of a conventional slot waveguide together with the slow-light enhancement from the 1D PC. Its simple geometry makes it resistant to fabrication imperfections and helps reduce the propagation loss, while still maintaining the benefit of large mode overlap and slow-light enhancement. Using it as a phase shifter and converting the phase shift to amplitude modulation through a Mach–Zehnder interferometer (MZI) structure, we demonstrate an integrated silicon-organic hybrid EO modulator. The observed effective EO coefficient is as high as 490 pm/V at 1562 nm wavelength. The measured half-wave voltage and length product is 0.91 V · cm, and can be further improved by adding narrow connecting arms [11]. The proposed structure offers a competitive novel phase-shifter design, which is compact, simple, highly efficient, and with low optical loss, for on-chip silicon-organic hybrid EO modulators.

The structure of the 1D PC slot waveguide is shown in Fig. 1. It is formed by a conventional slot waveguide with periodic rectangular teeth on its rails. The structural parameters of the 1D PC slot are chosen to support single-mode propagation while achieving high group index (slow light) around the optical wavelength of 1550 nm. The period (P) of the rectangular teeth is 415 nm. The width (a) and length (b) of the teeth are 124.5 nm ($0.3P$) and 300 nm, respectively. The slot has a width (S_w) of 150 nm and a rail width (R_w) of 100 nm. The 1D PC slot waveguide sits on top of a silicon dioxide layer and is covered with EO polymer (SEO 125 Soluxra, LLC., $n = 1.63$). Figure 2(a) shows the simulated photonic band diagram of the quasi-transverse-electric (TE) modes of the 1D PC slot waveguide using the 3D plane-wave expansion method. The nearly flat region of the lowest band is chosen as the operating range. It supports propagation mode in the PC slot waveguide and has a high group index ($n_g > 40$) close to the band edge [as shown in the inset of Fig. 2(a)]. The electric field intensity distribution of the mode at the band edge is shown in Figs. 2(b)–2(d). Optical power is strongly confined in the slot, and the ratio of the optical power in the EO polymer region is calculated to be $\sigma = 0.35$.

The 1D PC slot waveguide is accessed through conventional slot waveguides. To compensate the mode mismatch and improve coupling efficiency at the interface of the conventional slot waveguide and the 1D PC slot waveguide, a coupler is designed. Instead of using an adiabatically tapered long coupler [19], a very short intermediate low-group-index coupler (step taper) is used [20]. The schematic of the step taper is shown in Fig. 3(a). The optimized step taper consists of five periods of PC slot waveguides with shorter teeth ($b_T = 200$ nm) and slightly larger period ($P_T = 425$ nm). The width of the teeth remains unchanged ($a_T = 0.3P_T$, 127.5 nm). The parameters of the step taper (period P_T, tooth length b_T and width a_T, number of periods N) were optimized by transmission spectrum simulation using the 3D finite-difference time-domain (FDTD) method. Parts of the optimization process are shown in Figs. 3(b)–3(d). In Fig. 3(b), a_T, b_T and N are fixed, while P_T is scanned from 420 to 430 nm. Similarly, in Figs. 3(c) and 3(d), b_T and N are scanned separately. In this way, the optimized parameters for the step taper are determined. Figure 3(e) compares the simulated transmission before and after implementing the optimized step taper. It can be seen from the figure that the large fluctuations resulting from the group index mismatch has been significantly reduced by the short step taper (total length ~2 μm), and the additional loss caused by the taper is negligible. Finally, the conventional slot waveguide is connected to a strip waveguide through an s-shape strip-to-slot mode converter [21]. Figure 3(f) shows the measured transmission spectrum of a 200 μm long 1D PC slot waveguide filled with EO polymer. A clear band edge can be observed near 1550 nm.

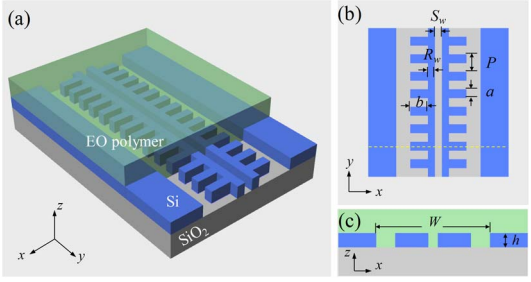

Fig. 1. (a) Schematic of the proposed 1D PC slot waveguide filled with EO polymer as a phase shifter for EO modulators. (b) and (c) are the top view and the cross-section view of the structure, respectively.

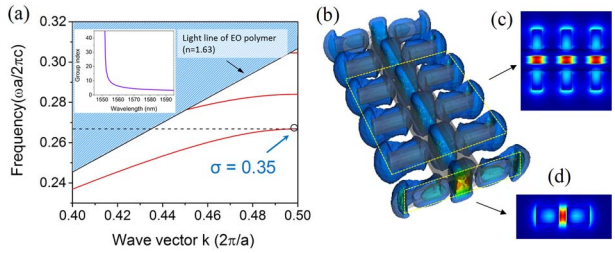

Fig. 2. (a) Band diagram of the 1D PC slot waveguide. Inset shows the mode profile at the band edge of the lowest band. (b)–(d) Mode profile at the band edge of the lowest band.

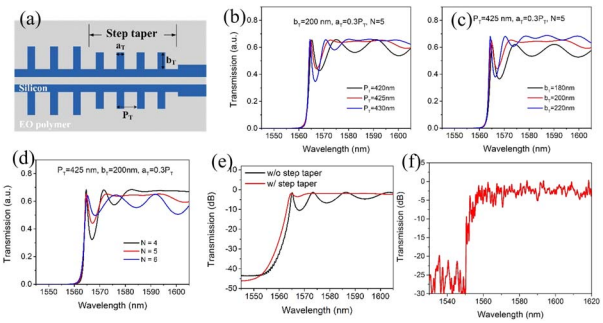

Fig. 3. (a) Schematic of the step taper; (b)–(d) simulated transmission spectrum of a 1D PC slot waveguide with step taper of (b) different periods (P_T), (c) different teeth length (b_T), and (d) different number of periods (N); (e) simulated transmission spectrum comparing 1D PC slot waveguide with (red curve) and without (black curve) step taper; (f) measured transmission spectrum of 1D PC slot waveguide with optimized step taper.

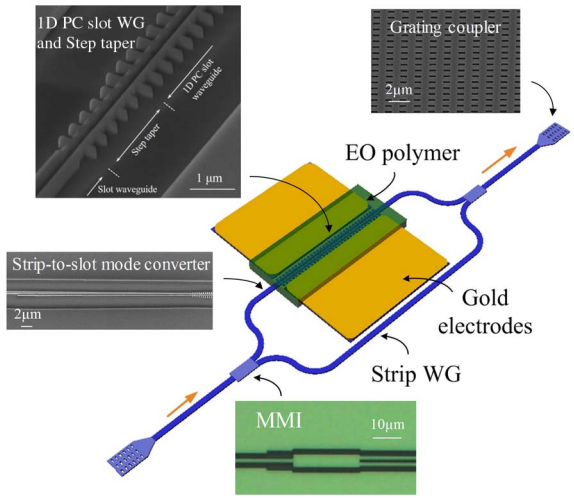

Fig. 4. Schematic of a MZI modulator based on 1D PC slot waveguide. Insets show SEM images of the waveguides and the grating coupler, and a microscopic image of the MMI.

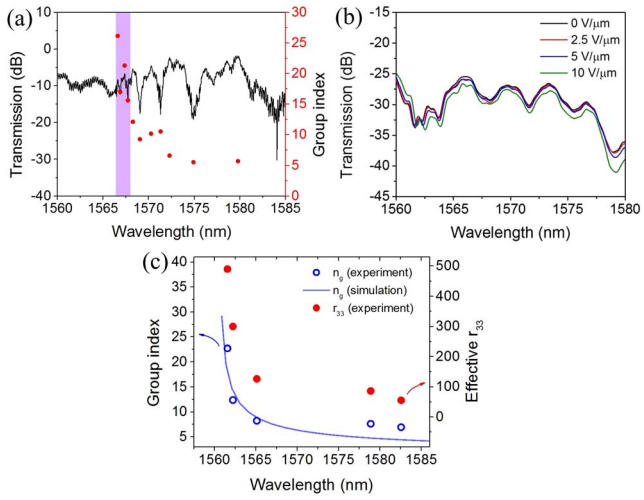

Fig. 5. (a) Measured transmission spectrum of the MZI structure and derived group index as a function of wavelength; (b) measured transmission spectra of the MZI modulator with different DC electric fields applied on the electrodes; (c) group index (from both simulation and experiment) and effective r_{33} as a function of wavelength.

To characterize the 1D PC slot waveguide as the phase shifter for modulators, an MZI structure was designed with one arm loaded with a 200 μm long 1D PC slot waveguide, as illustrated in Fig. 4. The proposed 1D PC slot waveguide, along with all connecting strip waveguides, 1 by 2 multimode interferometer (MMI), and subwavelength grating couplers [22], were patterned by e-beam lithography on a silicon-on-insulator (SOI) chip with a 250 nm thick top silicon layer. The pattern was then transferred onto the silicon layer through a single reactive ion etching (RIE) step. Gold electrodes were formed by photolithography, e-beam evaporation, and lift-off process. The gap size between the two electrodes is 4 μm. The insets of Fig. 4 show the scanning electron microscope (SEM) images of the fabricated silicon PC slot waveguide, strip-to-slot mode converter and grating coupler, and also the microscopic image of the MMI up to the above steps. Finally, the EO polymer was coated on the PC slot waveguide and cured overnight under vacuum at 80°C. It ensures that the polymer infiltrates the PC slot structures thoroughly, as shown in Ref. [15]. Before modulation measurement, the EO polymer goes through a poling process at its glass transition temperature of 150°C, with an external electric field of 100 V/μm applied through the gold electrodes. The poling process aligns the chromophores in the same direction in the host polymer and activates its EO effect.

Transmission spectra of the fabricated device were obtained from a testing platform using a broadband amplified spontaneous emission (ASE) source (1510–1630 nm) and an optical spectrum analyzer. Light from the ASE source was guided through a polarizer to subwavelength grating couplers and excited the fundamental quasi-TE mode of the on-chip strip waveguides. The transmission spectrum of the unbalanced MZI without applying any voltage on the electrodes was first measured and is shown in Fig. 5(a). The oscillations in the spectra are due to the group velocity difference between the two arms of the MZI. The oscillation period decreases rapidly at the band edge of the 1D PC slot waveguide, approximately 1567 nm. The group index therefore can be estimated from the oscillation patterns using the equation [23]

$$n_g^{\mathrm{pcw}}(\lambda) = n_g^{\mathrm{ref}}(\lambda) + \frac{\lambda_{\min}\lambda_{\max}}{2L(\lambda_{\min} - \lambda_{\max})}, \quad (1)$$

where n_g^{pcw} is the group index of the 1D PC slot waveguide, n_g^{ref} is the group index of the reference strip waveguide ($n_g^{\mathrm{ref}} = 4.2$), $\lambda_{\min}$ and $\lambda_{\max}$ are the wavelength at adjacent valley and peak of the oscillations, and $L = 200$ μm is the length of the phase shifter. The estimated group indices are drawn in the same plot. A group index over 25 is observed. The slow-light region has a width of about 1.5 nm (marked with color), with an average group index around 20, and can be improved by dispersion engineering [15]. The total loss of the MZI structure is ~10 dB, which includes propagation loss of the 200 μm 1D PC slot waveguide (~3 dB), coupling loss on the step taper (~3 dB), mode converter (~2 dB), and MMI (~2 dB). The propagation loss in the 1D PC slot is estimated at about 15 dB/mm. This loss is higher than a conventional slot waveguide filled with EO polymer (4 dB/mm) [10] due to scattering at the periodic structure, but is smaller than the 2D PC slot waveguide under similar fabrication conditions. The much simpler structure of 1D periodic teeth along the slot waveguide reduces the scattering loss, which is a major source of loss in real devices, and makes the device more impervious to fabrication imperfections.

To characterize the device performance, an electric field was applied on the phase shifter through the electrodes. Figure 5(b) shows the transmission spectra under different electric fields generated by DC voltage. The spectra show red shifts with increasing electric field from 0 to 10 V/μm. The phase shift induced by the applied electric field can be estimated from the equation $\Delta\varphi = 2\pi\Delta\lambda/\mathrm{FSR}$, where FSR is the free spectral range of the oscillations in the MZI spectrum. The half-wave voltage, which is the applied voltage when $\Delta\varphi = \pi$, is estimated according to the relationship between applied voltage and wavelength shift obtained from the spectra. Based on these equations, EO modulation efficiency ($V_\pi L$) of 0.91 V · cm is calculated near the wavelength of 1562 nm. The effective EO

coefficient of the EO polymer, $r_{33\text{eff}}$, can then be estimated by [14]

$$r_{33\text{eff}} = \frac{\lambda W}{n^3 V_\pi \sigma L}, \quad (2)$$

where $n = 1.63$ is the refractive index of the EO polymer, σ is the ratio of optical mode power in the EO polymer, and W is the gap size between the electrodes. The estimated $r_{33\text{eff}}$ near 1562 nm is 490 pm/V. This high r_{33} value is a result of the enhancement effect of the slow group velocity of the waveguide mode. Figure 5(c) shows the group index and effective EO coefficient as a function of wavelength in the same diagram. The increasing $r_{33\text{eff}}$ with increasing group index confirms that the effective EO coefficients, and thus modulation efficiencies are enhanced by the slow-light effect in our proposed PC slot waveguide.

In order to study the potential of phase-shifter designs comprehensively, we define a figure-of-merit $f = \sigma \cdot n_g \cdot L_{3\,\text{dB}}$, where σ is the ratio of optical mode in the EO polymer region, n_g is the group index in the waveguide, and $L_{3\,\text{dB}}$ is the length of the phase shifter in millimeters with 3 dB propagation loss. This figure-of-merit reflects a phase shifter's ability to efficiently confine and modulate the propagation mode in the waveguide. In our proposed 1D PC slot structure, $f = 0.35 \times 20 \times 0.2 \sim 1.4$, considering the 15 dB/mm propagation loss. In conventional slot waveguide-based EO modulators, like the ones in Refs. [10,11,13], $f \sim 0.4 \times 2 \times 0.75 \sim 0.6$, considering a typical propagation loss of 4 dB/mm when filled with EO polymer [10]. In a 2D PC slot waveguide [14,16], σ and n_g are similar to our proposed 1D PC waveguide, but the $L_{3\,\text{dB}}$ is smaller due to the larger scattering loss from the 2D PC structure. It can be seen that in a 1D PC slot waveguide, the slow-light effect provides more benefits than the extra propagation loss it induces, while the overlap factor is as high as that in conventional slot waveguides. Therefore, the proposed 1D PC slot waveguide has the potential to enable better efficiency in EO modulators compared to those based on conventional slot waveguides or 2D PC slot waveguides.

The above measurement results demonstrate the slow-light enhancement in the proposed structure. However, this modulator is not optimized for low voltage, high extinction ratio, and high-speed operation. To further reduce the half-wave voltage, it is feasible to use a strip-loaded structure [12] or to add narrow contacting arms to the PC teeth and connect the bulk silicon under the electrodes [11]. A push-pull configuration will help both lower the operating voltage and improve the extinction ratio. Considering high-speed operation, the silicon slabs between the electrodes and the slot filled with EO polymer is similar to a RC circuit, where the 3 dB frequency bandwidth can be estimated by $1/2\pi RC$. Through finite element simulation, the 3 dB bandwidth is about 61 GHz ($R = 6.9\ \text{k}\Omega$, $C = 0.38$ fF). To make the most out of the ultrafast response time of EO polymer material, the silicon slab can be properly doped to further reduce the equivalent resistance and improve the bandwidth [10,15]. With these additional considerations, the silicon-organic hybrid modulator has the potential of high-speed operation of tens of Gbit/s or even higher [7,10,24].

In summary, we have designed a slow light slot waveguide that has a simple 1D PC structure and demonstrated its enhancement effect in an MZI EO modulator. The proposed structure provides a new platform for applications that require maximum light-matter interaction within a short length, especially for on-chip silicon-organic hybrid EO modulators.

Funding. Air Force Research Laboratory (AFRL) (FA8650-14-C-5006, FA9550-16-C-0033).

[†]These authors contributed equally to this Letter.

REFERENCES

1. G. Reed, G. Mashanovich, F. Gardes, and D. Thomson, Nat. Photonics **4**, 518 (2010).
2. L. Liao, D. Samara-Rubio, M. Morse, A. Liu, D. Hodge, D. Rubin, U. D. Keil, and T. Franck, Opt. Express **13**, 3129 (2005).
3. W. M. Green, M. J. Rooks, L. Sekaric, and Y. A. Vlasov, Opt. Express **15**, 17106 (2007).
4. B. Bortnik, Y.-C. Hung, H. Tazawa, B.-J. Seo, J. Luo, A. K.-Y. Jen, W. H. Steier, and H. R. Fetterman, IEEE J. Sel. Top. Quantum Electron. **13**, 104 (2007).
5. Y. Enami, C. T. Derose, D. Mathine, C. Loychik, C. Greenlee, R. A. Norwood, T. D. Kim, J. Luo, Y. Tian, A. K.-Y. Jen, and N. Peyghambarian, Nat. Photonics **1**, 180 (2007).
6. M. Lee, Science **298**, 1401 (2002).
7. J. Leuthold, W. Freude, J. Brosi, R. Baets, P. Dumon, I. Biaggio, M. L. Scimeca, F. Diederich, B. Frank, and C. Koos, Proc. IEEE **97**, 1304 (2009).
8. F. Qiu, A. M. Spring, D. Maeda, M. Ozawa, K. Odoi, A. Otomo, I. Aoki, and S. Yokoyama, Sci. Rep. **5**, 8561 (2015).
9. C. Haffner, W. Heni, Y. Fedoryshyn, J. Niegemann, A. Melikyan, D. L. Elder, B. Baeuerle, Y. Salamin, A. Josten, U. Koch, C. Hoessbacher, F. Ducry, L. Juchli, A. Emboras, D. Hillerkuss, M. Kohl, L. R. Dalton, C. Hafner, and J. Leuthold, Nat. Photonics **9**, 525 (2015).
10. R. Palmer, S. Koeber, D. L. Elder, M. Woessner, W. Heni, D. Korn, M. Lauermann, W. Bogaerts, L. Dalton, W. Freude, J. Leuthold, and C. Koos, J. Lightwave Technol. **32**, 2726 (2014).
11. T. Baehr-Jones, B. Penkov, J. Huang, P. Sullivan, J. Davies, J. Takayesu, J. Luo, T. D. Kim, L. Dalton, A. Jen, M. Hochberg, and A. Scherer, Appl. Phys. Lett. **92**, 163303 (2008).
12. R. Ding, T. Baehr-Jones, Y. Liu, R. Bojko, J. Witzens, S. Huang, J. Luo, S. Benight, P. Sullivan, J.-M. Fedeli, M. Fournier, L. Dalton, A. Jen, and M. Hochberg, Opt. Express **18**, 15618 (2010).
13. R. Palmer, L. Alloatti, D. Korn, P. C. Schindler, R. Schmogrow, W. Heni, S. Koenig, L. Bolten, T. Wahlbrink, M. Waldow, H. Yu, W. Bogaerts, P. Verheyen, G. Lepage, M. Pantouvaki, J. Van Campenhout, P. Absil, R. Dinu, W. Freude, C. Koos, and J. Leuthold, IEEE Photon. J. **5**, 6600907 (2013).
14. X. Wang, C.-Y. Lin, S. Chakravarty, J. Luo, A. K.-Y. Jen, and R. T. Chen, Opt. Lett. **36**, 882 (2011).
15. X. Zhang, A. Hosseini, S. Chakravarty, J. Luo, A. K.-Y. Jen, and R. T. Chen, Opt. Lett. **38**, 4931 (2013).
16. C. Y. Lin, X. Wang, S. Chakravarty, B. S. Lee, W. Lai, J. Luo, A. K. Y. Jen, and R. T. Chen, Appl. Phys. Lett. **97**, 093304 (2010).
17. S. Inoue and A. Otomo, Appl. Phys. Lett. **103**, 171101 (2013).
18. A. Di Falco, M. Massari, M. G. Scullion, S. A. Schulz, F. Romanato, and T. F. Krauss, IEEE Photon. J. **4**, 1536 (2012).
19. C.-Y. Lin, A. X. Wang, W.-C. Lai, J. L. Covey, S. Chakravarty, and R. T. Chen, Opt. Lett. **37**, 232 (2012).
20. A. Hosseini, X. Xu, D. N. Kwong, H. Subbaraman, W. Jiang, and R. T. Chen, Appl. Phys. Lett. **98**, 031107 (2011).
21. X. Zhang, H. Subbaraman, A. Hosseini, and R. T. Chen, Opt. Express **22**, 20678 (2014).
22. X. Xu, H. Subbaraman, J. Covey, D. Kwong, A. Hosseini, and R. T. Chen, Appl. Phys. Lett. **101**, 031109 (2012).
23. Y. A. Vlasov, M. O'Boyle, H. F. Hamann, and S. J. McNab, Nature **438**, 65 (2005).
24. M. Hochberg, T. Baehr-Jones, G. Wang, M. Shearn, K. Harvard, J. Luo, B. Chen, Z. Shi, R. Lawson, P. Sullivan, A. K. Y. Jen, L. Dalton, and A. Scherer, Nat. Mater. **5**, 703 (2006).

128.67.43.205 {ts '2016-12-14 15:52:48'}